Role of the calcium-binding protein parvalbumin in short-term synaptic plasticity

Olivier Caillard*†, Herman Moreno‡, Beat Schwaller§, Isabel Llano*, Marco R. Celio§, and Alain Marty*

*Max-Planck-Institute for Biophysical Chemistry, D37 077 Göttingen, Germany; ‡New York University, New York, NY 10016; and §Institute of Histology and General Embryology, CH 1705 Fribourg, Switzerland

GABAergic (GABA = γ-aminobutyric acid) neurons from different brain regions contain high levels of parvalbumin, both in their soma and in their neurites. Parvalbumin is a slow Ca^{2+} buffer that may affect the amplitude and time course of intracellular Ca^{2+} transients in terminals after an action potential, and hence may regulate short-term synaptic plasticity. To test this possibility, we have applied paired-pulse stimulations (with 30- to 300-ms intervals) at GABAergic synapses between interneurons and Purkinje cells, both in wild-type (PV+/+) mice and in parvalbumin knockout (PV−/−) mice. We observed paired-pulse depression in PV+/+ mice, but paired-pulse facilitation in PV−/− mice. In paired recordings of connected interneuron-Purkinje cells, dialysis of the presynaptic interneuron with the slow Ca^{2+} buffer EGTA (1 mM) rescues paired-pulse depression in PV−/− mice. These data show that parvalbumin potently modulates short-term synaptic plasticity.

GABA | cerebellum | basket cells | stellate cells | Purkinje cells

The immediate consequences of past neuronal activity on synaptic strength are often examined by measuring the ratio (called paired-pulse ratio, or PPR) between the mean synaptic current in response to a test stimulation over that obtained with a conditioning stimulus. If the PPR is larger than 1, the synapse is considered as facilitating, whereas values smaller than 1 are characteristic of depressing synapses. However, facilitation and depression presumably coexist in all experimental conditions, and the PPR that is measured may be viewed as a balance between these two competing processes (1, 2).

Current hypotheses link facilitation to the fact that some of the Ca^{2+} ions entering the presynaptic terminal during the first stimulus are still present when the second stimulus is delivered (3, 4). Several modes of action have been envisaged for the residual calcium. It could act by binding to high affinity sites of the normal exocytosis machinery (5), by binding to special sites responsible for facilitation (2, 6), or by modulating the degree of saturation of high affinity Ca^{2+} buffers (7, 8), but direct evidence in favor of any of these possibilities is still lacking.

Depression is a complex phenomenon including both pre- and postsynaptic components. It may involve depletion of a readily releasable pool of vesicles, saturation or desensitization of postsynaptic receptors, or still other processes (7, 9).

Calcium-binding proteins such as parvalbumin (PV), calretinin, and calbindin D_{28k} are important modulators of intracellular calcium dynamics in neurons (10) and could therefore influence both facilitation and depression. Effects of these calcium buffers are determined by their affinities for Ca^{2+} ions and by the kinetics (on and off rates) of binding and releasing of Ca^{2+}. PV is in this regard interesting because it has a slow dissociation rate (about 1 s^{-1}) and a slow apparent association rate (about 10^7 M^{-1}·s^{-1}), due to the fact that Mg^{2+} ions compete with Ca^{2+} ions for binding. As a result of this situation, PV tends to accelerate the initial phase of decay of Ca^{2+} transients rather than slowing it down, as fast buffers would (11, 12). Furthermore PV reduces the peak calcium transients much less efficiently than fast buffers

do (11, 12). Specific subclasses of GABAergic (GABA = γ-aminobutyric acid) neurons from different brain regions contain high levels of PV both in their soma and in their processes, but the physiological role of PV in brain neurons remains unclear (10, 13, 14).

In the present work, we took advantage of the recent development of a strain of PV-deficient (PV−/−) mice (15) to investigate the effects of PV on short-term synaptic plasticity, using a PPR protocol. PV−/− mice have a locomotor behavior that can be distinguished from wild-type mice and show an increased susceptibility toward epileptic seizures¶. Because PV is highly expressed in axons and terminals of cerebellar interneurons [basket and stellate cells (14)], we centered our investigation on the synapse formed between these interneurons and Purkinje cells.

Materials and Methods

Immunohistochemistry. Sagittal cerebellar slices (100 μm thick) were prepared as described previously (18) and then fixed for 1 h with paraformaldehyde in PBS. Sections were incubated overnight with the rabbit PV antiserum PV-28 (Swant, Bellinzona, Switzerland), diluted 1:50 in PBS. After rinsing with PBS containing 1% albumin, sections were incubated with the secondary antibody (fluorescein anti-rabbit; Vector Laboratories) diluted 1:500 at 4°C in a dark room. Immunoreactive neurons were then visualized with a confocal microscope (Axiovert 135TV; Zeiss), using an illumination wavelength of 488 nm.

Western Blot Detection of PV in the Cerebellum. Brains were removed from killed mice and separated into forebrain and cerebellum. An approximately 5-fold larger volume of PBS (pH 7.4) containing 2 mM EDTA and a protease inhibitor mixture (Roche, Mannheim, Germany) was added, and the tissue was disrupted by using a Polytron Homogenizer (Kinematica, Lucerne, Switzerland). The suspension was centrifuged at 15,000 × g for 30 min at 4°C, and protein concentration of the supernatant was determined by using the Bradford assay (Bio-Rad). Proteins were separated by SDS/PAGE (15% polyacrylamide), trans-

ferred to Zeta probe-membranes (Bio-Rad), and immunostained with the antiserum PV4064 (1:1000) as described before (19). PV-immunoreactive bands were visualized by using 4-chlornaphthol/hydrogen peroxide as a chromogen. A parallel gel was stained with Coomassie blue to check for even loading.

ELISA. The sandwich ELISA for PV is very similar to the one published in detail for calretinin (20, 21). ELISA plates were pretreated with the monoclonal mouse anti-PV antibody PV235 (Swant; 0.2 mg/ml in bidistilled water, diluted 1:50 in 100 mM NaHCO$_3$, pH 8.0) for 16–24 h at room temperature. After blocking additional protein binding sites, purified recombinant PV or brain samples were added to the wells. Standard curves (0–5 ng/ml PV) were established with purified PV. After incubation for 24 h at room temperature with the detection antibody rabbit anti-PV antiserum PV28 (Swant), diluted 1:800 with buffer A, plates were processed as described previously (21).

Electrophysiology. Electrophysiological experiments were performed by using sagittal cerebellar slices (180 μm thick), which were prepared as described previously (18). Animal age ranged from 7 to 12 days.

Slices were perfused (1.5 ml/min) with an extracellular saline containing (in mM) 125 NaCl, 2.5 KCl, 1.25 NaH$_2$PO$_4$, 26 NaHCO$_3$, 2 CaCl$_2$, 1 MgCl$_2$, and 10 glucose. NBQX (10 μM) and D-AP5 (50 μM) were added to block α-amino-3-hydroxy-5-methyl-4-isoxazolepropionic acid (AMPA)-kainate and *N*-methyl-D-aspartate (NMDA) receptors respectively.

Tight-seal whole cell recordings were used to record inhibitory postsynaptic currents (IPSCs). The intracellular saline for Purkinje cells contained (in mM): 150 CsCl, 4.6 MgCl$_2$, 10 Hepes, 4 Na-ATP, 0.4 Na-GTP, 1 EGTA, and 0.1 CaCl$_2$. Series resistances ranged from 4 to 9 MΩ and were partially compensated (60–90%). Cell potential was held at -60 mV. All recordings were performed at room temperature.

Extracellular Stimulations. The stimulating electrode was a glass pipette of similar size to those used for patch-clamp of Purkinje cells, filled with a Hepes-buffered extracellular saline solution. The reference electrode for the stimulation circuit was made with a platinum wire wrapped around the stimulating electrode. A voltage pulse (10–60 V) or a current pulse (100–800 μA) was applied through the electrode during 50–200 μs. Special precautions were taken to maximize the chances that data represented reliable stimulations of a single presynaptic cell. The stimulation electrode was placed at various locations in the molecular layer, and a series of increasing stimulations were applied until single eIPSCs were evoked. If a clear intensity threshold to evoke an eIPSC was found, with an apparently stable response past the threshold, the location of the stimulating pipette was considered as satisfactory and the PPR measurements begun. The stimulation intensity was then set at 1.5$\times$ the value of the threshold. This procedure ensured that both the first and the second stimulus in a PPR protocol elicited a spike in the presynaptic neuron, without any failure.

Paired Recordings. Tight-seal whole-cell recordings of stellate or basket cells located in the vicinity of the recorded Purkinje cell were performed. The standard intracellular saline for interneurons contained (in mM): 150 K-gluconate, 4.6 MgCl$_2$, 10 Hepes, 4 Na$_2$-ATP, 0.4 Na$_2$-GTP, and 0.05 EGTA. In some experiments a higher buffer power was used (1 EGTA, 0.1 CaCl$_2$). Another variant of the interneuron intracellular solution (low Mg^{2+} solution) contained (in mM): 150 K-gluconate, 10 Hepes, 1.5 Mg-ATP, 2.5 Na$_2$-ATP 0.4 Na$_2$-GTP, and 0.05 EGTA. Pipette resistances as measured in the extracellular saline solution were on the order of 20 MΩ. Interneurons were kept in voltage-clamp

mode by using a holding potential of -60 mV. Axonal action potentials were triggered by depolarizing steps [test potential: $+10$ mV; duration: 5 ms (22)]. No attempt was made to compensate capacitive or leakage currents in the presynaptic recordings that are displayed in the figures. If the interneuron and the Purkinje cell were synaptically connected, IPSCs were evoked in the Purkinje cell, and the experiment could begin. Otherwise, the interneuron was discarded, and a new pair was tried. PPRs were determined by applying double stimulations at a frequency of 0.02 Hz.

Typical center-to-center distances between the somata of pre- and postsynaptic cells were 40–140 μm. Under these conditions, small ions reach the presynaptic terminals within tens of seconds (23). However due to the pipette-terminal solution exchange, irreversible decay of the synaptic strength occurs after an initial stable period of 5–10 min (23, 24). In addition, we were concerned by the possibility that PV could wash out of the terminals, a process that was expected to occur on a time scale of 10 min or more (based on considerations outlined in ref. 25). Therefore, the PPR was measured over a period of 1–10 min after the start of the presynaptic whole-cell recording. The PPR was stable during this time window.

Analysis. The PPR was defined as the ratio of the mean peak amplitudes of the two IPSCs. When the two IPSCs overlapped, the amplitude of the second IPSC was corrected by using a monoexponential fit to the decay of the first IPSC. All data are expressed as mean $\pm$ SEM. Statistical comparisons of PPRs were done with an ANOVA test. Data were considered significantly different when $P \leq 0.05$.

Results

Expression of PV in the Cerebellum of PV+/+, PV+/− and PV−/− Mice. The expression of PV was examined by immunohistochemistry in parasagittal sections of the cerebellum. In PV+/+ mice, a strong staining of the Purkinje cell bodies and dendrites was evident, and interneurons of the molecular layer (basket and stellate cells) were even more strongly labeled (Fig. 1*A*). No staining could be observed in the granule cell layer with the rare exception of few Purkinje cell axons. In PV-deficient mice, with similar parameters of excitation, no signal at all could be detected in any of the cerebellar layers (not shown); a very faint staining of Purkinje-cell somata and dendrites, probably reflecting a nonspecific background staining, could be observed when increasing the image contrast (Fig. 1*B*).

Western blot analysis of the cytosolic cerebellar fractions from the three genotypes (PV+/+, PV+/−, and PV−/−) revealed a reduced signal in PV+/− mice and a complete lack of signal in PV−/− mice (Fig. 1*C*). The results were further supported by a quantitative ELISA assay. PV levels were 8.7 $\pm$ 1.6 μg/mg of protein in PV+/+ mice and 3.4 $\pm$ 0.6 in PV+/− mice (40% compared with PV+/+), and no detectable levels were measured in PV−/− mice. The results from Western blot analysis and ELISA are in agreement with previous studies on fast-twitch muscles where no detectable levels of PV could be found in PV-deficient mice (15).
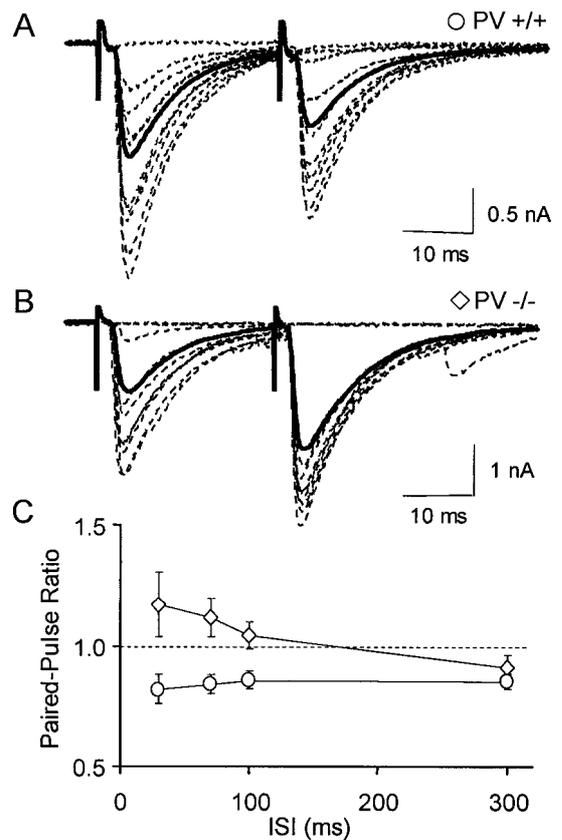
Extracellular Stimulations. To record interneuron-evoked IPSCs (eIPSCs), whole-cell recordings were obtained in Purkinje cells. Double pulses were applied through an extracellular pipette located in the lower part of the molecular layer to stimulate the axons of stellate or basket cells. Interstimulus intervals (ISIs) ranged from 30 to 300 ms. For ISIs shorter than 30 ms, eIPSCs overlap heavily. We did not study PPRs at such short ISIs to avoid complications due to possible postsynaptic effects (9). In PV+/+ mice, the amplitude of the second eIPSC was smaller than that of the first for ISIs ranging from 30 to 300 ms (Fig. 2*A*). The PPR was 0.84 $\pm$ 0.05 at 30 ms and 0.86 $\pm$ 0.04 at 100 ms ($n =$
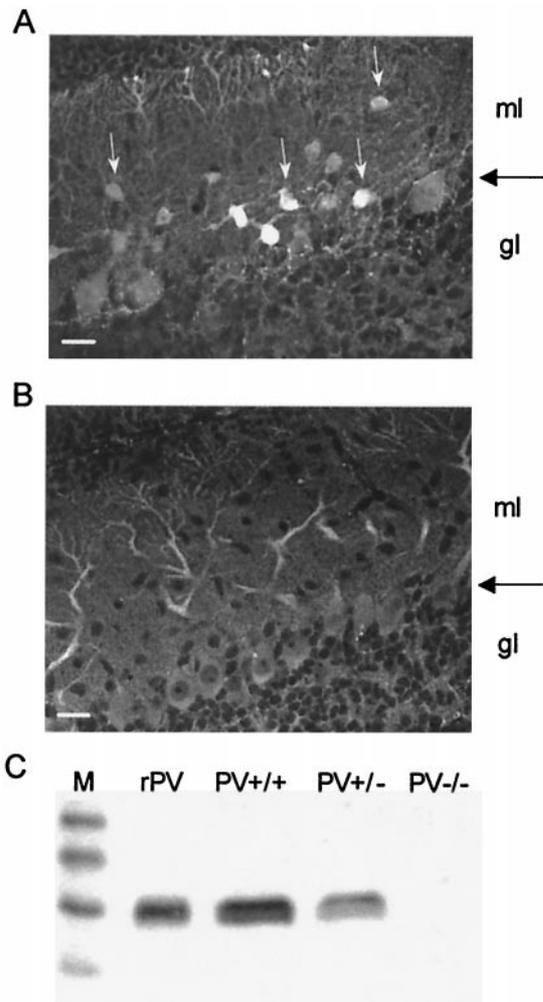
Fig. 1. Expression of PV in the cerebellum. (A) Immunohistochemical staining of a cerebellar slice (sagittal cut) from a PV+/+ mouse (P8). The Purkinje cell layer is marked by a large horizontal arrow. PV-ir interneurons are localized in the molecular layer (ml; white arrows). No PV-ir cells are found in the granule cell layer (gl). Dendritic trees of Purkinje cells extending into two thirds of the molecular layer are also stained. Scale bar = 25 μm. (B) A cerebellar slice from a PV−/− mouse (P11) stained under identical conditions does not show any specific PV immunoreactivity. Contrast was greatly increased in comparison to A. (C) Western blot from cerebellar protein extracts reveal a clear signal in PV+/+ mice, a reduced one in PV+/−, and no detectable signal in PV−/− animals. rPV, recombinant rat PV as positive control; M, marker proteins (sizes in kDa from top to bottom: 31, 21, 14, and 7).

Fig. 2. Absence of paired-pulse depression in PV−/− mice. (A) Superimposed IPSCs recorded in a Purkinje cell of a PV+/+ mouse after double extracellular stimulations of GABAergic interneurons (30ms ISI, dotted traces), and average response for the entire experiment (solid trace). (B) Representative results from a similar experiment performed with a PV−/− mouse. (C) Average PPR as a function of ISI in PV+/+ mice (circles, $n = 12$) and PV−/− mice (diamonds, $n = 19$). Note that, in this figure and in the following ones, failures are included in the calculation of mean traces.

12 cells; Fig. 2C). Application of the GABA$_B$ antagonist CGP55845A (1 μM) did not modify the PPR ($n = 7$, $P = 0.84$), indicating that the PPR was independent of the activation of presynaptic GABA$_B$ receptors. These results show that interneuron-Purkinje cell synapses are depressing in control juvenile mice, as they are in juvenile rats (26). In PV−/− mice, however, the mean amplitude of the second eIPSC was larger than that of the first one for ISIs ranging from 30 to 100 ms. PPR values were 1.17 ± 0.08 at 30 ms and 1.04 ± 0.05 at 100 ms ($n = 19$ cells; Fig. 2 B and C). By comparison to the PV+/+ mice, the PPR was significantly different at 30-, 70-, and 100-ms ISI. These results indicate that, for ISIs of 100 ms or less, elimination of PV converts depressing synapses into facilitating ones.

Paired Recordings. To gain further insight into the mechanisms responsible for the PPR changes, we compared the properties of GABAergic synapses in PV−/− and PV+/+ mice by using

connected pairs (stellate cell-Purkinje cell or basket cell-Purkinje cell). This method had two advantages over extracellular stimulation. First, possible changes in release probability could be evaluated by analyzing failure rates. Secondly, manipulations of the presynaptic Ca^{2+} buffer could be attempted. We were in particular interested to see whether adding EGTA to the presynaptic cell in PV−/− mice could rescue the PV+/+ phenotype. EGTA was selected for these rescue experiments because it is, like PV, a slow Ca^{2+} buffer (11, 12, 27).

After the switch to whole-cell configuration in the interneuron, pairs of depolarizing steps were applied under somatic voltage clamp. This protocol led to the generation of action potentials that propagated along the axon (22) and gave rise to an eIPSC when the recorded Purkinje cell was synaptically connected.

In the PV−/− pairs, when the interneuron was recorded with a low concentration of EGTA (50 μM; standard presynaptic solution), the PPRs measured at 30 ms and 70 ms ISI were 1.22 ± 0.05 and 1.14 ± 0.11, respectively ($n = 13$, Fig. 3 A and C). The PPRs measured in these conditions were similar to the ones measured when interneurons were extracellularly stimulated. In contrast, when the interneuron was recorded with 1 mM EGTA, the PPRs measured at 30 ms and 70 ms ISI were 0.94 ± 0.04 and 1.01 ± 0.1, respectively (Fig. 3 B and C). At 30 ms ISI the PPR was significantly lower than the one measured with extracellular stimulation or with a low EGTA concentration. In the PV−/−
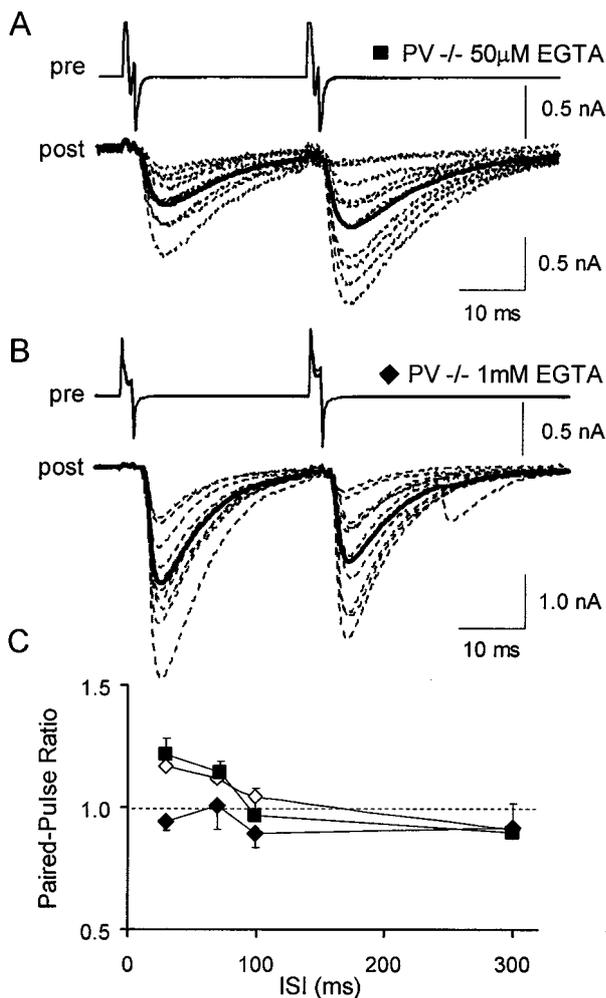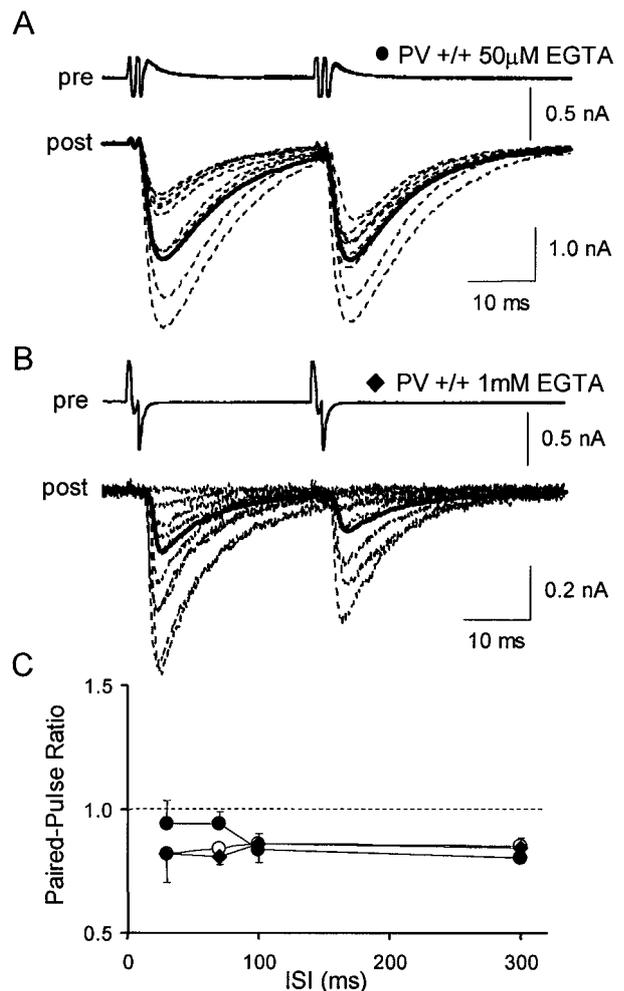
Fig. 3. Paired-pulse depression can be rescued in PV−/− mice by EGTA. (*A*) Superimposed IPSCs recorded in a Purkinje cell (dotted traces, post) of a PV−/− mouse after induction of two action potentials in a presynaptic interneuron by depolarizing steps (30 ms ISI) and average response for the entire experiment (solid trace). The interneuron was recorded with a solution containing 50 μM EGTA. (*B*) Representative results from a similar experiment where the interneuron was recorded with a solution containing 1 mM EGTA. (*C*) Average PPR as a function of ISI in PV−/− mice in conditions where interneurons were extracellularly stimulated (open diamonds, same data as in Fig. 2C), or were recorded with a solution containing 50 μM EGTA (filled squares, *n* = 13), or were recorded with a solution containing 1 mM EGTA (filled diamonds, *n* = 11).

Fig. 4. Effect of presynaptic dialysis of EGTA in PV+/+ mice. (*A*) Superimposed IPSCs recorded in a Purkinje cell (dotted traces, post) of a PV+/+ mouse after induction of two action potentials in a presynaptic interneuron by depolarizing steps (30 ms ISI) and average response for the entire experiment (solid trace). The interneuron was recorded with a solution containing 50 μM EGTA. (*B*) Representative results from a similar experiment where the interneuron was recorded with a solution containing 1 mM EGTA. (*C*) Average PPR as a function of ISI in PV+/+ mice in conditions where interneurons were extracellularly stimulated (open circles, same data as in Fig. 2C), or were recorded with a solution containing 50 μM EGTA (filled circles, *n* = 11), or were recorded with a solution containing 1 mM EGTA (filled diamonds, *n* = 9).

pairs, the percentage of failure was not significantly modified by EGTA [8 ± 3% with 50 μM EGTA and 6 ± 5% with 1 mM EGTA (*P* = 0.74)].

These data show that the switch from paired-pulse depression to paired-pulse facilitation in the PV−/− can be reversed by dialyzing EGTA into the presynaptic interneuron. Furthermore, the failure data suggest that addition of a slow buffer such as EGTA does not modify the release probability.

In PV+/+ pairs, when the interneurons were recorded with the standard solution (with 50 μM EGTA), the PPRs measured at 30 ms and 70 ms were 0.94 ± 0.05 (*n* = 11) and 0.94 ± 0.06 (*n* = 6, Fig. 4). These values are much lower than the corresponding values in PV−/− mice, but they are slightly higher than those obtained with extracellular stimulation in PV+/+ mice. When the interneurons were recorded with 1 mM EGTA in PV+/+ experiments, the PPRs measured at 30 ms and 70 ms

dropped to 0.82 ± 0.03 (*n* = 9) and 0.81 ± 0.08 (*n* = 7), respectively, that is, to values very close to the ones measured with extracellular stimulation. The percentage of failures with 50 μM EGTA was not significantly different from that in 1 mM EGTA (14 ± 4% instead of 12 ± 5%; *P* = 0.83).

These results indicate that, in PV+/+ mice, as in PV−/− mice, addition of EGTA to presynaptic neurons shifts the PPR to lower values without affecting the failure rate of the first IPSC. In PV+/+ paired experiments, a difficulty arises from the fact that the high affinity Ca^{2+}-binding sites of PV also have a moderately high affinity for Mg^{2+} such that PV under basal intracellular Ca^{2+} is largely in the Mg^{2+}-bound form (28). If the Mg^{2+} concentration chosen for the pipette does not match that of the cytosol, establishment of the new Mg^{2+} concentration on presynaptic whole-cell recording will change the buffering power of PV. Physiological values of the resting free Mg^{2+} concentration $[Mg^{2+}]_i$ in neurons are around 300 μM (29). Because

NEUROBIOLOGY

Table 1. Properties of the basket/stellate cells-Purkinje cells connections

	PV				
	+/+			−/−	
Property	0.050 mM, $[EGTA]_i$ 730 μM, $[Mg^{2+}]_i$	0.050 mM, $[EGTA]_i$ 50 μM, $[Mg^{2+}]_i$	1 mM, $[EGTA]_i$ 730 μM, $[Mg^{2+}]_i$	0.050 mM, $[EGTA]_i$ 730 μM, $[Mg^{2+}]_i$	1 mM, $[EGTA]_i$ 730 μM, $[Mg^{2+}]_i$
Amplitude, nA	0.48 ± 0.13 (13)	0.61 ± 0.16 (6)	0.54 ± 0.19 (10)	0.51 ± 0.18 (13)	1.99 ± 0.53 (11)
Failure, %	13 ± 5 (13)	6 ± 4 (6)	13 ± 5 (10)	9 ± 4 (13)	6 ± 5 (11)
Var/mean, pA	110 ± 46 (13)	93 ± 21 (6)	87 ± 19 (10)	98 ± 22 (13)	144 ± 27 (11)

Numbers in parentheses indicate the numbers of paired recordings in each condition. The last line indicates the variance-to-mean ratio of peak IPSCs in each condition.

$[Mg^{2+}]_i$ was relatively high in our standard intracellular solution (estimated at 730 μM, assuming a K_d for ATP and GTP of 0.1 mM (30)), we performed additional experiments with an interneuron solution containing 50 μM EGTA and an estimated $[Mg^{2+}]_i$ of 50 μM. In these conditions, the PPR at 30 ms ISI was 0.85 ± 0.06, a value somewhat lower than that found with 730 μM, and very close to those obtained with extracellular stimulation. Even though the difference between 50 μM and 730 μM results did not reach significance at the $P < 0.05$ level ($P = 0.25$), the close agreement between the former results and those obtained with extracellular stimulation suggests that the true value of $[Mg^{2+}]_i$ is closer to 50 μM than to 730 μM.

Overview of IPSC Properties in PV+/+ and PV−/− Mice. Basic parameters of eIPSCs in paired recordings appear in Table 1. Mean IPSCs were not different among the groups, apart from an anomalous high value in PV−/− pairs with 1 mM EGTA, for which we have presently no satisfactory explanation. Failure rates and variance to mean ratios did not show significant differences among groups. Overall, these results suggest that the main features of synaptic transmission, as assayed with single pulse protocols, were not strongly modified by PV deletion or by alterations of the presynaptic Mg^{2+} or EGTA concentration.

Fig. 5 recapitulates the PPR results obtained with ISIs of 30 ms. The PPRs fall in 3 categories: (*i*) low values around 0.85 (all in PV+/+ mice; experiments by using extracellular stimulations, paired recordings with 1 mM EGTA, or paired recordings with 50 μM EGTA and low Mg^{2+}); (*ii*) intermediate values near 0.95 (paired recordings of PV+/+ mice with 50 μM EGTA and high Mg^{2+}, or paired recordings of PV−/− mice with 1 mM EGTA); (*iii*) and high values near 1.20 (PV−/− mice, either with extracellular stimulations or with paired recordings by using 50 μM EGTA).

Discussion

The principal results of this study are that elimination of PV changes a depressing synapse into a facilitating one, and that adding back EGTA in PV−/− mice restores the wild-type phenotype.

Slow buffers such as EGTA affect transmitter release after an unconditioned stimulus only if release sites are not in direct vicinity to the site of Ca^{2+} influx, the voltage-dependent Ca^{2+} channels (8). In some preparations [squid giant synapse (27) and pyramidal-pyramidal synapses (31)], where influx and release are apparently tightly coupled together, EGTA does not inhibit markedly the probability of release, whereas in other preparations [crayfish neuromuscular junction (32) or hippocampal mossy fiber synapse (33, 34)], where the coupling is looser, a significant reduction is observed. Our finding that the probability of failures is not different in PV+/+ and in PV−/− strains, and that it is not modified by addition of EGTA in PV−/− mice (Table 1), suggests that the interneuron-Purkinje cell synapse falls in the first category, where release sites are closely associated to voltage-dependent Ca^{2+} channels.

The effects of EGTA and PV on the PPR may be understood by considering their effects on the Ca^{2+} transient on a time scale of milliseconds, i.e., after the collapse of channel-associated Ca^{2+} domains. EGTA or PV do not reduce markedly the peak Ca^{2+} transient resulting from voltage-dependent Ca^{2+} influx, but they accelerate the initial rate of decay of this transient (11, 12, 35). The acceleration of the Ca^{2+} decay is likely to reduce the residual Ca^{2+} concentration and hence to inhibit facilitation (35). The effects on the PPR due to the elimination of PV and of its replacement with EGTA are in agreement with this expectation. Examination of the time course of the PPR in the various experimental conditions suggests that it is facilitation, not depression, that is modified. Facilitation decays as a function of the ISI within a few hundreds of milliseconds (1, 35, 36), whereas recovery from depression typically has a time constant of one or several seconds (1, 37). We find that the effects of PV deletion or of EGTA addition on the PPR decay quickly with the ISI; these effects are maximal at an ISI of 30 ms and are very weak or absent for an ISI of 300 ms (Figs. 2*C*, 3*C*, and 4*C*). The nearly constant depression found at 300 ms independently of the presence of PV or EGTA suggests that these buffers do not modify significantly the extent of depression. By a similar reasoning, the fact that the PPR slowly grows with the ISI
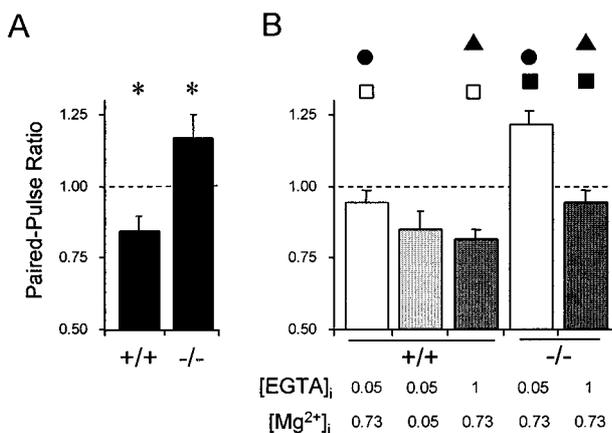
Fig. 5. Average PPR at 30 ms ISI in different experimental conditions. (*A*) Average PPR at 30 ms ISI in PV+/+ (n = 12) and in PV−/− mice (n = 19). The interneurons were stimulated by using an extracellular stimulation. The PPRs are significantly different (asterisks). (*B*) Average PPR at 30 ms ISI in paired recordings. The interneurons were stimulated by depolarizing steps in whole-cell voltage-clamp configuration. The presynaptic recording solution contained different concentrations of EGTA or Mg^{2+}. Significant differences can be observed between PV+/+ and PV−/− for two different presynaptic solutions (dots and triangles). Both in PV+/+ and in PV−/− mice, the PPR is significantly reduced by increasing the concentration of EGTA (open and filled squares).

throughout the 30- to 300-ms range in the wild type (Fig. 2*C*) suggests that, in this condition, facilitation is negligible.

Thus, our results are most simply explained by assuming that PV and EGTA specifically and completely inhibit facilitation. Both buffers act presumably by reducing the residual Ca^{2+} prevalent at the time of the second stimulus. Note that the effect of a given buffer on the PPR depends critically on the binding kinetics of the buffer to Ca^{2+}. If the binding is rapid, the synaptic response to the first stimulus will be reduced, so that the extent of depression expected from vesicle deprivation will be decreased. Furthermore, the residual Ca^{2+} present at the time of the second stimulus will tend to saturate the fast buffer, leading to facilitation (7, 8). Thus, addition of a fast buffer is expected to lead to an increased PPR, and, conversely, removal of a fast buffer should decrease the PPR. Calbindin D_{28k}, which is a significantly faster buffer than PV (38), but still has a binding rate for calcium about 10-times smaller than 1,2-bis(2-aminophenoxy)ethane-*N*,*N*,*N'*,*N'*-tetraacetic acid (BAPTA), could act as a slow buffer or as a fast buffer depending on the preparation and the stimulation protocol. In hippocampal neurons in culture, addition of calbindin reduces posttetanic potentiation (39), and, in these conditions, calbindin acts like a slow buffer. However, at hippocampal mossy fiber synapses, removal of calbindin leads to reduced facilitation, so that here calbindin appears to act as a fast buffer (40).

With 730 μM Mg^{2+}, adding 1 mM EGTA in PV$-/-$ mice restored the same PPR as that obtained in PV$+/+$ mice with 50 μM EGTA (Fig. 5). This result indicates that the speed of Ca^{2+} removal is the same for 950 μM EGTA and for the (unknown) concentration of PV prevailing in PV$+/+$ mice. Because the dissociation rate constants of Ca^{2+}-EGTA and Ca^{2+}-PV, 0.3 s^{-1} (41) and 1 s^{-1} (12), respectively, are small compared with the inverse of the ISI (33 s^{-1}), the rate of Ca^{2+} decay is determined by the rate of binding of Ca^{2+} to the buffers. Assuming apparent binding rates of 2.7×10^6 M^{-1}·s^{-1} for EGTA (42) and of 4.3×10^6 M^{-1}·s^{-1} for PV [calculated assuming a value of 730 μM for $[Mg^{2+}]_i$, according to (12)], it may be calculated that the concentration of PV in PV$+/+$ mice is 600 μM. This is a large value, which is however in line with the earlier estimate of 1 mM obtained with immunogold staining in axons and presynaptic terminals of cerebellar stellate and basket cells (14). With a concentration of this order of magnitude, it is hardly surprising that PV exerts potent effects on short-term synaptic plasticity in this preparation.

A striking correlation was found in various brain regions (hippocampus, neostriatum, and frontal cortex) between the presence of PV and the firing pattern of neurons: unlike other GABAergic neurons, PV-containing neurons are always able to fire repetitively at a high rate (10, 43, 44). In line with this correlation, we note that cerebellar stellate and basket cells fire in bursts at high rate *in vivo* (16). The present results, together with previous ones (11, 12), suggest two ways by which the presence of PV in the presynaptic neuron could contribute to maintain synaptic transmission during bursts. First, PV helps bringing down the presynaptic Ca^{2+} quickly, thus preventing the potentially deleterious effects of excessive Ca^{2+} accumulation in the presynaptic cell. Second, PV maintains the strength of the synapse near its resting level by preventing cumulative facilitation, thus permitting nearly linear information processing in the postsynaptic neuron as a function of action potential number. It should be pointed out, however, that the removal of facilitation would work only as long as the incoming Ca^{2+} does not saturate PV. Thus, for prolonged bursts at high rates of firing, presynaptic Ca^{2+} accumulation and postsynaptic facilitation are expected to reappear (12), unless depression takes the lead (17, 37).

1. Debanne, D., Guerineau, N. C., Gähwiler, B. H. & Thompson, S. M. (1996) *J. Physiol. (London)* **491,** 163–176.
2. Dittman, J. S., Kreitzer, A. C. & Regehr, W. G. (2000) *J. Neurosci.* **20,** 1374–1385.
3. Zucker, R. S. (1989) *Annu. Rev. Neurosci.* **12,** 13–31.
4. Zucker, R. S. (1999) *Curr. Opin. Neurobiol.* **9,** 305–313.
5. Bertram, R., Sherman, A. & Stanley, E. F. (1996) *J. Neurophysiol.* **75,** 1919–1931.
6. Yamada, W. M. & Zucker, R. S. (1992) *Biophys. J.* **61,** 671–682.
7. Neher, E. (1998) *Neuron* **20,** 389–399.
8. Neher, E. (1998) *Cell Calcium* **24,** 345–357.
9. Jones, M. V. & Westbrook, G. L. (1996) *Trends Neurosci.* **19,** 96–101.
10. Baimbridge, K. G., Celio, M. R. & Rogers, J. H. (1992) *Trends Neurosci.* **15,** 303–308.
11. Chard, P. S., Bleakman, D., Christakos, S., Fullmer, C. S. & Miller, R. J. (1993) *J. Physiol. (London)* **472,** 341–357.
12. Lee, S. H., Schwaller, B. & Neher, E. (2000) *J. Physiol. (London)* **525,** 419–432.
13. Celio, M. R. (1990) *Neuroscience* **35,** 375–475.
14. Kosaka, T., Kosaka, K., Nakayama, T., Hunziker, W. & Heizmann, C. W. (1993) *Exp. Brain Res.* **93,** 483–491.
15. Schwaller, B., Dick, J., Dhoot, G., Carroll, S., Vrbova, G., Nicotera, P., Pette, D., Wyss, A., Bluethmann, H., Hunziker, W. & Celio, M. R. (1999) *Am. J. Physiol.* **276,** C395–C403.
16. Eccles, J. C., Llinas, R. & Sasaki, K. (1966) *Exp. Brain Res.* **1,** 1–16.
17. Galarreta, M. & Hestrin, S. (1998) *Nature Neuroscience* **1,** 587–594.
18. Llano, I., Marty, A., Armstrong, C. M. & Konnerth, A. (1991) *J. Physiol. (London)* **434,** 183–213.
19. Solbach, S. & Celio, M. R. (1991) *Anat. Embryol.* **184,** 103–124.
20. Schierle, G. S., Gander, J. C., Dorlando, C., Celio, M. R. & Weisenhorn, D. M. V. (1997) *Cereb. Cortex* **7,** 142.
21. Schwaller, B., Bruckner, G., Celio, M. R. & Hartig, W. (1999) *J. Neurosci. Methods* **92,** 137–144.
22. Tan, Y. P. & Llano, I. (1999) *J. Physiol. (London)* **520,** Part 1, 65–78.
23. Vincent, P. & Marty, A. (1996) *J. Physiol. (London)* **494,** 183–199.
24. Pouzat, C. & Marty, A. (1999) *J. Neurosci.* **19,** 1675–1690.
25. Pusch, M. & Neher, E. (1988) *Pflügers Arch.* **411,** 204–211.
26. Pouzat, C. & Hestrin, S. (1997) *J. Neurosci.* **17,** 9104–9112.
27. Adler, E. M., Augustine, G. J., Duffy, S. N. & Charlton, M. P. (1991) *J. Neurosci.* **11,** 1496–1507.
28. Eberhard, M. & Erne, P. (1994) *Eur. J. Biochem.* **222,** 21–26.
29. Stout, A. K., Li-Smerin, Y., Johnson, J. W. & Reynolds, I. J. (1996) *J. Physiol. (London)* **492,** 641–657.
30. Martell, A. & Smith, R. (1977) *Critical Stability Constants* (Plenum, New York), Vol. 2.
31. Ohana, O. & Sakmann, B. (1998) *J. Physiol. (London)* **513,** 135–148.
32. Winslow, J. L., Duffy, S. N. & Charlton, M. P. (1994) *J. Neurophysiol.* **72,** 1769–1793.
33. Castillo, P. E., Salin, P. A., Weisskopf, M. G. & Nicoll, R. A. (1996) *J. Neurosci.* **16,** 5942–5950.
34. Salin, P. A., Scanziani, M., Malenka, R. C. & Nicoll, R. A. (1996) *Proc. Natl. Acad. Sci. USA* **93,** 13304–13309.
35. Atluri, P. P. & Regehr, W. G. (1996) *J. Neurosci.* **16,** 5661–5671.
36. Wu, L. G. & Saggau, P. (1994) *J. Neurosci.* **14,** 645–654.
37. von Gersdorff, H., Schneggenburger, R., Weis, S. & Neher, E. (1997) *J. Neurosci.* **17,** 8137–8146.
38. Feher, J. J., Fullmer, C. S. & Wasserman, R. H. (1992) *Am. J. Physiol* **262,** C517–C526.
39. Chard, P. S., Jordan, J., Marcuccilli, C. J., Miller, R. J., Leiden, J. M., Roos, R. P. & Ghadge, G. D. (1995) *Proc. Natl. Acad. Sci. USA* **92,** 5144–5148.
40. Klapstein, G. J., Vietla, S., Lieberman, D. N., Gray, P. A., Airaksinen, M. S., Thoenen, H., Meyer, M. & Mody, I. (1998) *Neuroscience* **85,** 361–373.
41. Smith, P. D., Liesegang, G. W., Berger, R. L., Czerlinski, G. & Podolsky, R. J. (1984) *Anal. Biochem.* **143,** 188–195.
42. Naraghi, M. (1997) *Cell Calcium* **22,** 255–268.
43. Kawaguchi, Y. (1993) *J. Neurosci.* **13,** 4908–4923.
44. Kawaguchi, Y. & Kubota, Y. (1993) *J. Neurophysiol.* **70,** 387–396.

NEUROBIOLOGY